10-8-2016

Magnetic Reconnection With a Fast Perpendicular Sheared Flow

Xuanye Ma
University of Alaska, Fairbanks, max@erau.edu

Antonius Otto
University of Alaska, Fairbanks

Peter A. Delamere
University of Alaska, Fairbanks

Scholarly Commons Citation

Ma, X., Otto, A., & Delamere, P. A. (2016). Magnetic Reconnection With a Fast Perpendicular Sheared Flow. *Journal of Geophysical Research: Space Physics, 121*(10). https://doi.org/10.1002/2016JA023107

AGU PUBLICATIONS

JGR

Journal of Geophysical Research: Space Physics

RESEARCH ARTICLE
10.1002/2016JA023107

Magnetic reconnection with a fast perpendicular sheared flow

Xuanye Ma[1], Antonius Otto[1], and Peter A. Delamere[1]

[1]Geophysical Institute, University of Alaska Fairbanks, Fairbanks, Alaska, USA

Key Points:
- Magnetic reconnection with a fast perpendicular shear flow forms an expanding out flow region to maintain total pressure balance
- Plausible observational signatures in the outflow region include decreased density and pressure and increased magnetic field strength
- The boundary structure can be KH stable in three dimensions

Correspondence to:
X. Ma,
xma2@alaska.edu

Citation:
Ma, X., A. Otto, and P. A. Delamere (2016), Magnetic reconnection with a fast perpendicular sheared flow, *J. Geophys. Res. Space Physics*, *121*, 9427–9442, doi:10.1002/2016JA023107.

Received 23 JUN 2016
Accepted 9 SEP 2016
Accepted article online 15 SEP 2016
Published online 8 OCT 2016

Abstract Magnetic reconnection at the Earth's low-latitude magnetopause near the flank region is likely associated with a large sheared flow, being frequently quasi-perpendicular to the antiparallel magnetic field components. The magnitude of a fast sheared flow can be super-Alfvénic and even overcome the local fast mode speed. A scaling analysis implies a contradiction between the Walén relation and the balance of the total pressure for magnetic reconnection with a supercritical perpendicular sheared flow. This study uses one- and two-dimensional magnetohydrodynamic (MHD) simulations to demonstrate that the traditional reconnection layer violates the Walén relation but still maintains the total pressure balance in such a configuration. The results show an expanded outflow region, consistent with the presence of divergent normal flow, and a significant decrease of the plasma density as well as the thermal pressure in the outflow region. In contrast, the magnitude of the magnetic field in the outflow region matches the value in the inflow region due to the total pressure balance, which is fundamentally different from the classical reconnection layer under sub-Alfvénic perpendicular sheared flow conditions. In three-dimensional geometry, the fast sheared flow without being stabilized by the magnetic field is expected to be Kelvin-Helmholtz unstable. However, the three-dimensional MHD simulation suggests that such structure can be KH stable. Although, the presence of surface waves modulates some two-dimensional features, the major characteristics of the expanded outflow region are likely to be observed by in situ satellites.

1. Introduction

Sheared flows between the solar wind plasma and the magnetospheric plasma are fundamentally important for the solar wind coupling with magnetized planets (e.g., Earth, Saturn, and Jupiter). Different physical processes operate as a function of the sheared flow relative to the local typical speeds, that is, Alfvén speed, $V_A = B/\sqrt{\mu_0\rho}$, and ion acoustic speed, $C_s = \sqrt{\gamma p/\rho}$. Here B, ρ, μ_0, p, and $\gamma = 5/3$ are the magnetic field, plasma density, vacuum permeability, thermal pressure, and adiabatic index, respectively. Although the configuration of a large magnetic shear with a quasi-parallel sheared flow has been widely studied [*Chen*, 1997; *Cassak and Otto*, 2011], sheared flows are often quasi-perpendicular to the antiparallel magnetic field components, and the magnitude can be greater than the Alfvén speed. For instance, the magnitude of sheared flow near the Earth's magnetospheric tailward flank boundary is about 300∼1000 km s^{-1}, which is likely to be super-Alfvénic. The sheared flow on the dawn sides of Saturn's and Jupiter's magnetospheres can also be super-Alfvénic due to the fast corotating magnetodiscs. However, the configuration of large antiparallel magnetic field components with a super-Alfvénic perpendicular sheared flow has never been systemically studied.

For the case where the interplanetary magnetic field (IMF) is quasi-parallel to the planetary magnetic field, e.g., northward IMF conditions for the Earth's magnetosphere, nonlinear Kelvin-Helmholtz (KH) waves driven by a large sheared flow can form thin current layers, and consequently trigger magnetic reconnection [*Fairfield et al.*, 2000; *Otto and Fairfield*, 2000; *Nykyri and Otto*, 2001, 2004; *Nakamura et al.*, 2006; *Nykyri et al.*, 2006; *Nakamura et al.*, 2008]. As such, solar wind plasma can access the magnetosphere.

For the case where the IMF is quasi-antiparallel to the planetary field (e.g., southward IMF conditions for the Earth's magnetosphere), magnetic reconnection is considered as the dominant process. In two dimensions, the changes of the plasma properties (density, velocity, pressure, and magnetic field) from one inflow region through the outflow region to the other inflow region is mostly one-dimensional and is established through a series of magnetohydrodynamic (MHD) waves and discontinuities. Such a layer structure is called a reconnection layer [*Lin and Lee*, 1993]. For instance, in the traditional Petschek reconnection model, the inflow and outflow regions are divided by a pair of switch-off shocks [*Petschek*, 1964].

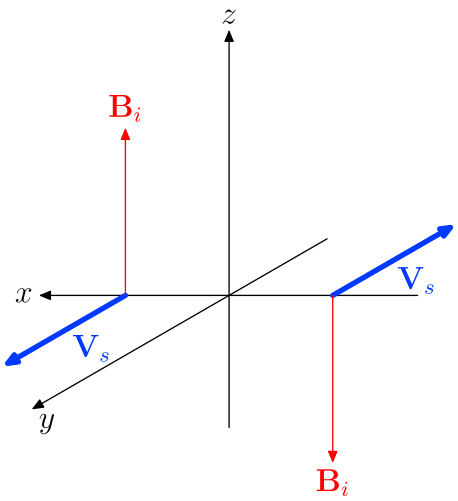

Figure 1. Sketch of the initial configuration.

At the Earth's magnetopause, the angle between the sheared flow, $\mathbf{V}_s$, and antiparallel magnetic field component, $\mathbf{B}$, is arbitrary. Thus, a systematic approach for addressing the question of how the presence of the sheared flow influences magnetic reconnection begins from the two limiting cases, that is, the parallel case ($\mathbf{V}_s \parallel \mathbf{B}$) and the transverse case ($\mathbf{V}_s \perp \mathbf{B}$).

For the parallel case, the condition is either KH unstable (i.e., $V_s > V_A$) [*Chandrasekhar*, 1961] or tearing mode unstable (i.e., $V_s < V_A$) [*Chen et al.*, 1997; *Cassak and Otto*, 2011]. Here V_s is the plasma sheared flow speed.

For the transverse case, one- and two-dimensional MHD simulations show that the pair of switch-off shocks in the Petschek reconnection model are replaced with a pair of slow shocks and a pair of rotational discontinuities (RDs) [*Sun et al.*, 2005]. From a three-dimensional perspective, reconnected magnetic field lines are dragged into opposite directions on the two sides of the outflow region due to the frozen-in condition, which consequently forms a magnetic field component perpendicular to the reconnection plane [*La Belle-Hamer et al.*, 1995]. For a resistive MHD system, the rotational discontinuity becomes a time-dependent intermediate shock (TDIS). This reconnection layer maintains the total pressure (i.e., thermal pressure and magnetic pressure) constant, that is,

$$p_{\text{tot}} = p_o + \frac{B_o^2}{2\mu_0} = p_i + \frac{B_i^2}{2\mu_0}, \tag{1}$$

where the subscripts o and i refer to the outflow region and inflow region, respectively. Meanwhile, TDIS/RT also follows the Walén relation [*Walén*, 1944], that is, the change of the velocity is equal to the change of the Alfvén speed, $\Delta V = \pm \Delta V_A$. Note that, for a symmetric configuration

$$V_s^2 = \frac{B_o^2}{\mu_0 \rho_o} < \frac{2p_{\text{tot}}}{\rho} = \frac{B_i^2}{\mu_0 \rho_i} + \frac{2p_i}{\rho_i} = V_{Ai}^2 + \frac{2}{\gamma} C_{si}^2 = V_c^2, \tag{2}$$

where V_s is the magnitude of sheared flow perpendicular to the antiparallel magnetic field B_i in the inflow region (please see Figure 1), B_o is the magnitude of the magnetic field in the outflow region, and the critical speed based on the total pressure is defined as $V_c = \sqrt{2p_{\text{tot}}/\rho} = \sqrt{V_{Ai}^2 + (2/\gamma)C_{si}^2}$. The equation (2) demonstrates that the classical reconnection layer, which maintains the total pressure balance and follows the Walén, only exists when the sheared flow, V_s, is smaller than the critical speed, $V_c = \sqrt{V_{Ai}^2 + (2/\gamma)C_{si}^2}$. For the configuration of supercritical perpendicular sheared flow (i.e., $V_s > V_c = \sqrt{V_{Ai}^2 + (2/\gamma)C_{si}^2}$), the balance of the total pressure, indicating the violation of the Walén relation, as we will demonstrate, is achieved by a fast expanding outflow region, which is fundamentally different from the classical reconnection layer.

One should also keep in mind, the one- and two-dimensional geometries limit the KH instability along the third dimension. The presence of the guide field (i.e., the magnetic field along the sheared flow direction) can stabilize the magnetopause boundary if the sheared flow speed is lower than the Alfvén speed associated with this guide field. As such, the magnetic reconnection layer, composed of a pair of slow shocks and

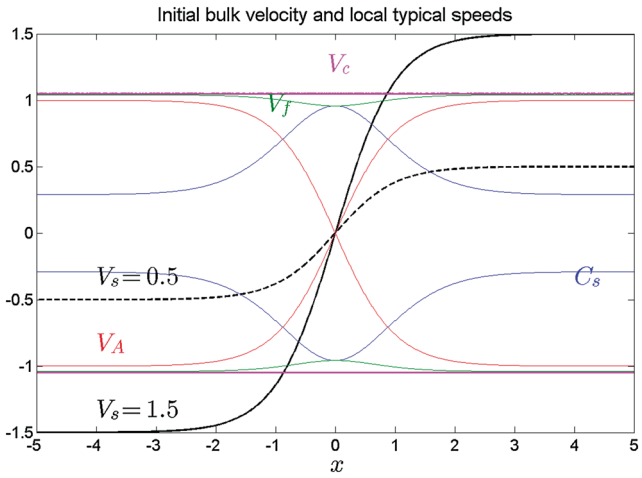

Figure 2. Profile of initial velocity for $V_s = 0.5$ (black dashed line), $V_s = 1.5$ (black solid line), Alfvén speed, $V_A = B/\sqrt{\rho}$ (red), ion acoustic speed, $C_s = \sqrt{\gamma/(2\rho)}$ (blue), fast mode speed, $V_f = \sqrt{C_s^2 + V_A^2}$ (green), and critical speed, $V_c = \sqrt{p_{\text{tot}}/\rho}$ (magenta) in our normalization (see in context).

RDs/TDISs, can still exist in three dimensions. In contrast, the magnetopause is KH unstable when the sheared flow speed is larger than the Alfvén speed along the sheared flow direction [*Chandrasekhar*, 1961]. Both magnetic reconnection and the KH instability can operate simultaneously [*Chen*, 1997]. The nonlinear interaction between the KH wave and magnetic reconnection has been discussed by *Ma et al.* [2014a, 2014b].

When the magnitude of the perpendicular sheared flow, V_s, is larger than the local fast mode speed, $V_f = \sqrt{V_A^2 + C_s^2}$, the sheared flow layer becomes KH stable again [*Miura and Pritchett*, 1982]. For a sheared flow parallel to the antiparallel magnetic field components, the velocity must be super-Alfvénic for the KH instability to operate and to switch reconnection off. For a sheared flow perpendicular to the antiparallel magnetic field components, magnetic reconnection and the KH instability can operate simultaneously up to supercritical sheared flow. For supercritical sheared flow, the KH instability is switched off and only reconnection can operate. However, the contradiction between the Walén relation and the balance of the total pressure indicates that the reconnection layer would be fundamentally different from the classical reconnection layer under sub-Alfvénic perpendicular sheared flow conditions. In this paper, the reconnection layer in such a configuration will be investigated in the frame of MHD by using one- and two-dimensional numerical simulations. Nevertheless, the presence of the magnetic reconnection layer changes the width of the sheared flow, as such the KH instability may operate at the late stage of the process. A key question is whether the major characteristics in one- and two-dimensional configurations can still exist in three dimensions, which will also be addressed in this study by using three-dimensional MHD simulation. The numerical simulation methods, results, and discussion will be presented in sections 2–4, respectively.

2. Numerical Methods

In this study we use a leap-frog scheme to numerically solve the full set of normalized resistive MHD equations [*Potter*, 1973; *Birn*, 1980; *Otto*, 1990]. All length scales, L, are normalized to the half width of the initial current layer, L_0; density, ρ, is normalized to the initial inflow density, $\rho_0 = n_0 m_0$, with the number density, n_0, and ion mass, m_0; the magnetic field, B, is normalized to the initial inflow magnetic field, B_0; the velocities, V, are measured in units of the Alfvén speed in the inflow region, $V_A = B_0/\sqrt{\mu_0 \rho_0}$, time, t, is normalized to Alfvén transit time, $\tau = L_0/V_A$, and the thermal pressure, p, is normalized to $B_0^2/(2\mu_0)$. As such, the magnetic pressure, the thermal pressure, and the total pressure, p_{tot}, are represented by B^2, p, and $B^2 + p$. Consequently, the acoustic speed, C_s, is $\sqrt{\gamma p/(2\rho)}$, and the critical speed, V_c, is $\sqrt{p_{\text{tot}}/\rho}$ in this normalization.

The whole set of simulations in this study is based on the same coordinate system, that is, the x direction is the normal direction of the current layer; the y direction is along the sheared flow direction, and the z direction is along the antiparallel magnetic field component (please see Figure 1). Thus, the reconnection geometry is confined to the x, z plane and three-dimensional effects through surface waves require the y direction.

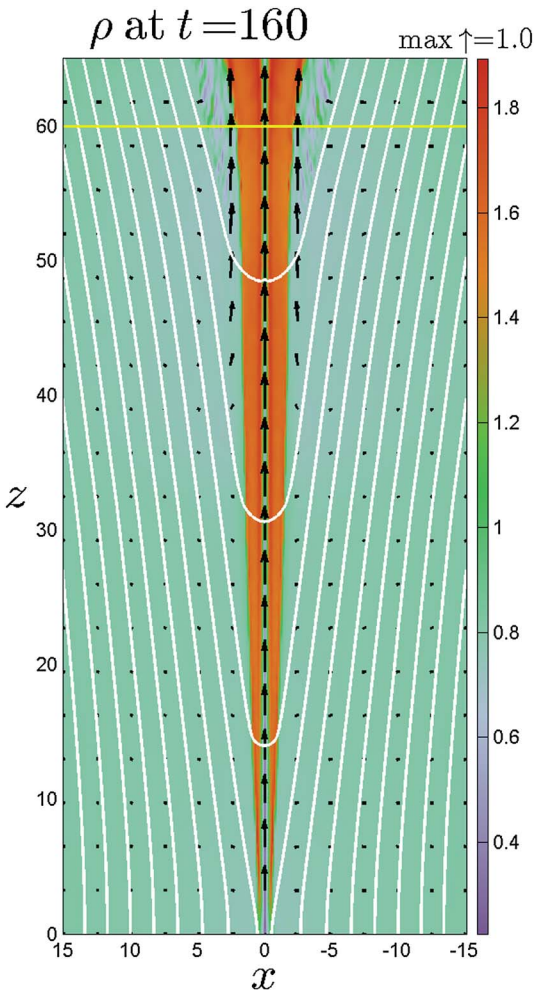

Figure 3. The plasma density (color index), the in-plane bulk velocity (black arrows), and magnetic field lines (white lines) for reconnection with a sub-Alfvénic perpendicular sheared flow (i.e., $V_s = 0.5$) at $t = 160$. The yellow line indicates the place where the one-dimensional line cut takes.

For this study, we focus on the simplest symmetric configuration. Thus, the initial one-dimensional steady state conditions used in the simulations are $\mathbf{V} = V_s \tanh(x)\hat{\mathbf{e}}_y$, $\mathbf{B} = \tanh(x)\hat{\mathbf{e}}_z$, $p = \cosh^{-2}(x) + p_\infty$, and $\rho = 1$. Here p_∞ is 0.1, meaning that the inflow plasma beta is 0.1, which is close to its typical value at the Earth's magnetopause. As such, the critical speed is $\sqrt{p_{\mathrm{tot}}/\rho} = \sqrt{1.1}$, and the fast mode speed is less than 1.04. We set V_s to be 0.5 and 1.5, representing the cases of sub-Alfvén speed (i.e., $V_s < V_f < V_c$) and superfast speed (i.e., $V_s > V_c > V_f$), respectively. The bulk velocity and the local typical speed are illustrated in Figure 2 for comparison.

We note that it may be academically interesting to discuss the configuration that the magnitude of sheared flow is between the fast mode speed and critical speed (i.e., $V_c > V_s \geq V_f$). Generally speaking, such a configuration is KH stable and the reconnection layer maintains the total pressure balance, expected to be identical to the two-dimensional configuration of reconnection with a sub-Alfvén perpendicular sheared flow. In practice, the typical plasma beta at the Earth's magnetopause is the order of unity, indicating that the fast mode speed, V_f, is almost identical to the critical speed, $V_c = \sqrt{V_{Ai}^2 + (2/\gamma)C_{si}^2}$. Therefore, we will not explore this case. We will also not address the critical case that the sheared flow speed is equal to the critical speed (i.e., $V_s = V_c = \sqrt{V_{Ai}^2 + (2/\gamma)C_{si}^2}$), since the conclusion based on such a specific parameter value may not have robust meaning. Furthermore, we do not have precise control of the inflow region, because the fast mode will slightly modulate the inflow region shortly after the process is triggered, as we will see in section 3. For this reason we set the sheared flow, V_s, well below or above the critical speed, $V_c = \sqrt{V_{Ai}^2 + (2/\gamma)C_{si}^2}$, to explore the two different configurations.

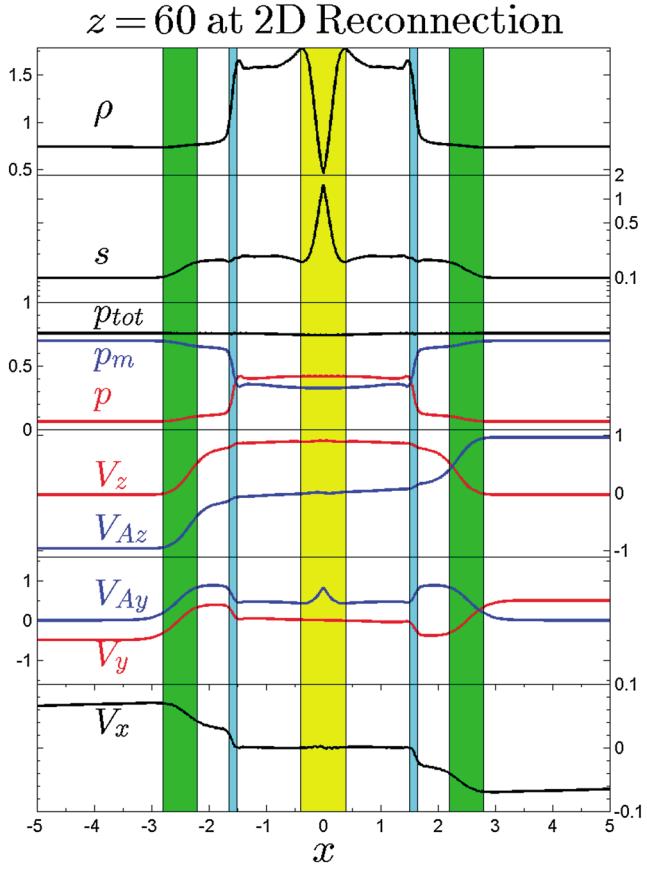

Figure 4. Profiles of the one-dimensional cut at $z = 60$ (i.e., yellow lines in Figure 3) for reconnection with a sub-Alfvénic perpendicular sheared flow (i.e., $V_s = 0.5$). The panels from top to bottom show (first panel) the plasma density and (second panel) the specific entropy, $s = p/\rho^{\gamma}$, (third panel) the total pressure, the thermal pressure, and the magnetic pressure, (fourth and fifth panels, respectively) the z and y component of the bulk velocity and the Alfvén speed, and (sixth panel) the x component of the bulk velocity. The pair of rotational discontinuities and slow shocks are highlighted by green and blue shading, respectively. The yellow shading highlights the density depletion layer.

Our study begins from two-dimensional simulations with a rectangular domain of $|x| < 30$ and $0 < z < 160$, which eliminates the influence of surface waves along the y direction. This large domain along the z direction allows a fully developed steady outflow region. Magnetic reconnection is triggered by a time-dependent localized resistivity model, i.e., $\eta = \eta_0[1 - \exp(-t/t_0)]\cosh^{-1}(x)\cosh^{-1}(z) + \eta_b$ [*Ma and Otto*, 2013], where the background resistivity is $\eta_b = 0.004$, and η_0 is 0.06. The nonuniform grids along the x and z directions provide the highest resolution of $\Delta x = \Delta z = 0.05$ in the diffusion region by using 603×803 grid points. Free boundary conditions ($\partial_n = 0$, where ∂_n represents the partial derivative in the direction normal to the boundary) are applied to the boundaries along the x direction and z maximum boundary. The z minimum boundary is determined by symmetry properties of the MHD equations [*Otto et al.*, 2007].

In general, the magnetic reconnection steady outflow region is a one-dimensional structure, which can be better resolved by solving the so called "one-dimensional Riemann problem" [*Lin and Lee*, 1993, 1999]. The initial steady state condition is the same as it is in the two-dimensional geometry, and this process can be triggered by adding a small constant magnetic $B_x = 0.025$ component [*Lin and Lee*, 1993, 1999; *Ma and Otto*, 2013]. The large simulation domain ($|x| < 80$) that is resolved by 3201 uniform grid points allows MHD waves to be fully developed without being influenced by the boundary conditions. A very small constant resistivity η of 2×10^{-4} is included in our simulations.

It is noticeable that a developed reconnection layer changes the width of sheared flow layer, which may form a KH unstable condition. Such possibilities are investigated by our three-dimensional simulations within a cubic domain of $|x| < 30$, $|y| < 20$, and $|z| < 40$. The x and z directions are resolved by 151 and 201 nonuniform grid points with a best resolution $\Delta x = \Delta z = 0.1$ in the vicinity of the center. The y direction is resolved by 201

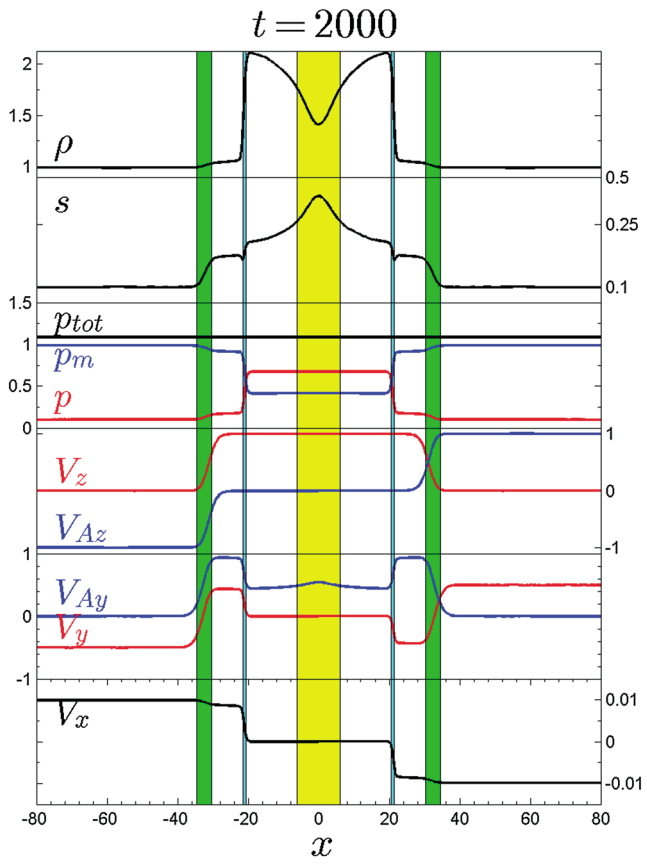

Figure 5. Same as Figure 4 except that it shows the reconnection layer for a sub-Alfvénic perpendicular sheared flow (i.e., $V_s = 0.5$) from one-dimensional simulation.

uniform grid points. Notice that the size of the *z* direction determines the longest KH wavelength mode in the system [*Ma et al.*, 2014a]. Thus, the simulation domain is chosen to correspond to a longest wavelength of 4 Earth radii, which is the typical KH wavelength at Earth's magnetopause near the flank region [*Fairfield et al.*, 2000; *Otto and Fairfield*, 2000; *Ma et al.*, 2014a]. Magnetic reconnection is triggered by a magnetic perturbation given by $\delta\mathbf{B} = \delta B f(y)\nabla A(x,z) \times \hat{\mathbf{e}}_y$, where magnetic flux $A(x,z) = \cosh^{-2}(x)\cosh^{-2}(z)$ is localized along the *y* direction by $f(y) = \frac{1}{2}[\tanh(\frac{y+5}{2}) - \tanh(\frac{y-5}{2})]$. This study uses a large perturbation $\delta B = 0.5$ to speed up the evolution to the nonlinear reconnection state. The three-dimensional simulations apply a current dependent resistivity, ensuring that the resistivity is very small almost everywhere except in the location where the current density is large (or equivalently, relative electron and ion drift speeds are large) [*Ma et al.*, 2014a, 2014b]. It has also been verified that the results are insensitive to the resistivity model [*Ma et al.*, 2014b]. We use open boundary conditions along the *x* and *z* directions and periodic boundary conditions along the *y* direction.

3. Results

The one- and two-dimensional configurations rule out the surface wave along the *y* direction (i.e., invariant direction for one- and two-dimensional configurations). Therefore, we present the results from one- and two-dimensional simulations in section 3.1 and separately discuss three-dimensional results in section 3.2.

3.1. Reconnection Without Surface Wave

3.1.1. Sub-Alfvénic Conditions ($V_s < V_c = \sqrt{V_{Ai}^2 + (2/\gamma)C_{si}^2}$)

We first consider the case of a sheared flow of magnitude 0.5 in order to provide typical conditions and a reference case for sheared flow perpendicular to the reconnection plane. Figure 3 shows the plasma density (color index), the in-plane bulk velocity (black arrows), and magnetic field lines (white lines) for reconnection with a sub-Alfvénic perpendicular sheared flow (i.e., $V_s = 0.5 < V_s = \sqrt{V_{Ai}^2 + (2/\gamma)C_{si}^2}$), showing a density depletion layer (blue area) embedded in the center of the narrow steady outflow region (red area).

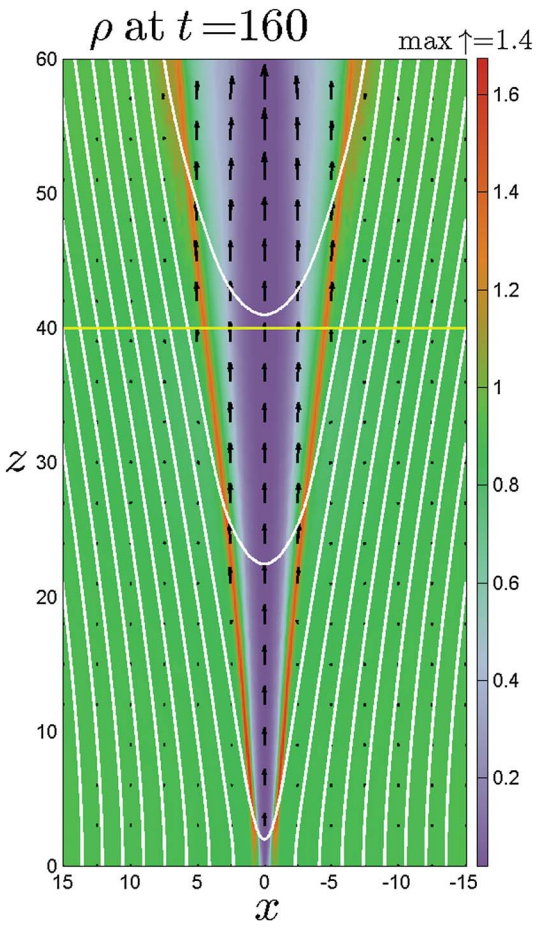

Figure 6. The plasma density (color index), the in-plane bulk velocity (black arrows), and magnetic field lines (white lines) for reconnection with a supercritical perpendicular sheared flow (i.e., $V_s = 1.5$) at $t = 160$. The yellow line indicates the place where the one-dimensional line cut is taken.

To better illustrate the reconnection layer structure, we take a one-dimensional line cut at $z = 60$ (yellow line in Figure 3). Figures 4 (first panel) to 4 (sixth panel) show the plasma density (first panel), the specific entropy, $s = p\rho^{-\gamma}$ (second panel), the total pressure, the thermal pressure, and the magnetic pressure (third panel), the z and y components of the bulk velocity and the Alfvén velocity (fourth and fifth panels, respectively), and the x component of the bulk velocity (sixth panel). The pair of TDISs and slow shocks is highlighted by green and blue shadings, respectively. The yellow shading highlights the density depletion layer. The total pressure curve demonstrates that this reconnection layer maintains the total pressure balance and the panels with the Alfvén and flow speed illustrate that the reconnection configuration satisfies the Walén relation (i.e., variations in V and V_A are identical). The bulk velocity V_x component indicates a convergent flow in the inflow region; however, it almost vanishes in the outflow region. The source of low density and high specific entropy plasma in the density depletion layer is the diffusion region [*Ma and Bhattacharjee*, 2001; *Ma and Otto*, 2014]. Therefore, the width of the density depletion layer is close to the width of the diffusion region (i.e., the ion or even electron inertia scales), being exaggerated in the MHD simulation. As such, the large specific entropy enhancement is likely insignificant because it fills only a very small volume based on the electron diffusion region width [*Ma and Otto*, 2014]. We note that the magnetic field and the density in the inflow region are slightly smaller than the initial condition, which is likely due to the modulation of the fast mode wave and numerical diffusion.

The almost identical reconnection layer structure can be found in one-dimensional simulations of the Riemann problem (see Figure 5). Note that the nonpropagating entropy structure (yellow shading) in Figure 5 only slightly increases the specific entropy (i.e., about 2 times), being much less than the specific entropy increase in the depletion layer in the two-dimensional configuration (i.e., about 1 order of magnitude).

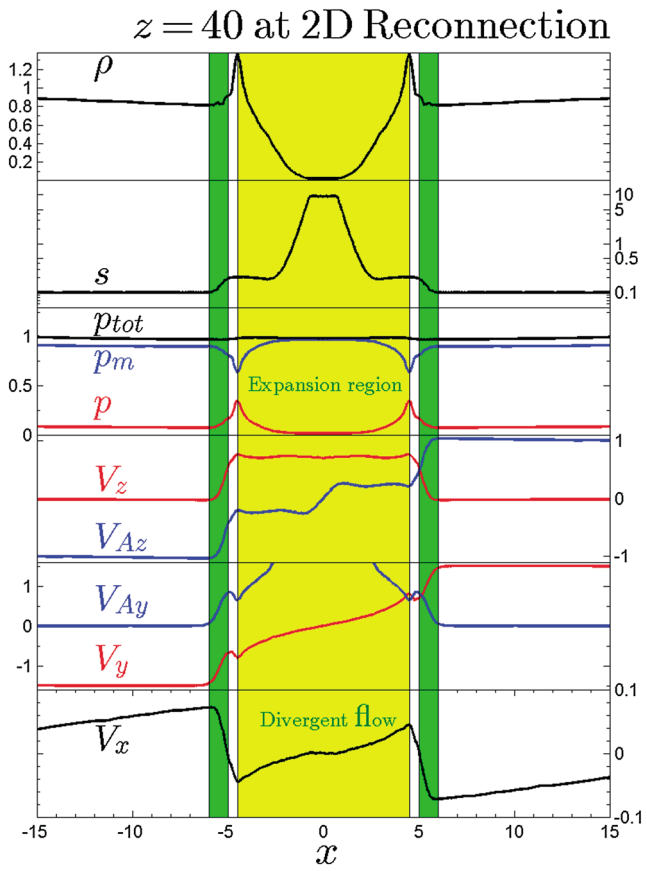

Figure 7. Same as Figure 4 except that it shows profiles of the one-dimensional cut at $z = 40$ (i.e., yellow lines in Figure 6) for magnetic reconnection with a supercritical perpendicular sheared flow (i.e., $V_s = 1.5$).

This is because the high specific entropy in the nonpropagating entropy structure in one dimension is a residue of the initial specific entropy rather than increasing by additional nonadiabatic heating.

3.1.2. Supercritical Conditions ($V_s > V_c = \sqrt{V_{Ai}^2 + (2/\gamma)C_{si}^2}$)

Figure 6 represents the plasma density (color index), the in-plane bulk velocity (black arrows), and magnetic field lines (white lines) for reconnection with a superfast perpendicular sheared flow (i.e., $V_s = 1.5 > V_c = \sqrt{V_{Ai}^2 + (2/\gamma)C_{si}^2}$) at $t = 160$. It shows an expanding density depletion layer (blue area) which is separated from the inflow region (green area) by a pair of compressed layers (red area). Figure 7 shows the profiles of a one-dimensional cut at $z = 40$ (i.e., yellow line in Figure 6). It shows that the reconnection layer is composed of a pair of TDISs (green shading) and an expansion region (yellow shading), which still maintains approximately total pressure balance; however, the Walén relation is only valid in the pair of TDISs. It is noticeable that the bulk velocity V_x component is convergent in the inflow region at the maximum speed of 0.075, and it is divergent in the outflow region at the maximum speed of 0.05. Such divergent flow decreases the plasma density in the outflow region and expands the density depletion layer. The flat region of plasma density in the outflow region indicates that density decreases to the low critical density ($\rho_c = 0.02$) in our simulation. Such low critical density is set to maintain the stability of the simulation. In reality, the plasma density will further decrease in this region. The specific entropy profile shows a slight enhancement through the TDIS and remains constant near the edges of the expansion region (i.e., $5 > |x| > 3$). The significant increase of specific entropy in the vicinity of the x axis is basically due to the expansion of the density depletion layer. The magnetic pressure increases in the expansion region, where the thermal pressure decreases, being opposite to the slow shock. The flow is convergent at the interface between TDIS and expansion region, which slightly compresses the plasma and forms the compressed layer (red region in Figure 6).

Figure 8 presents a very similar result from the one-dimensional simulation of the Riemann problem, basically showing a pair of TDISs and an expansion region. We note that the density still significantly decreases in the

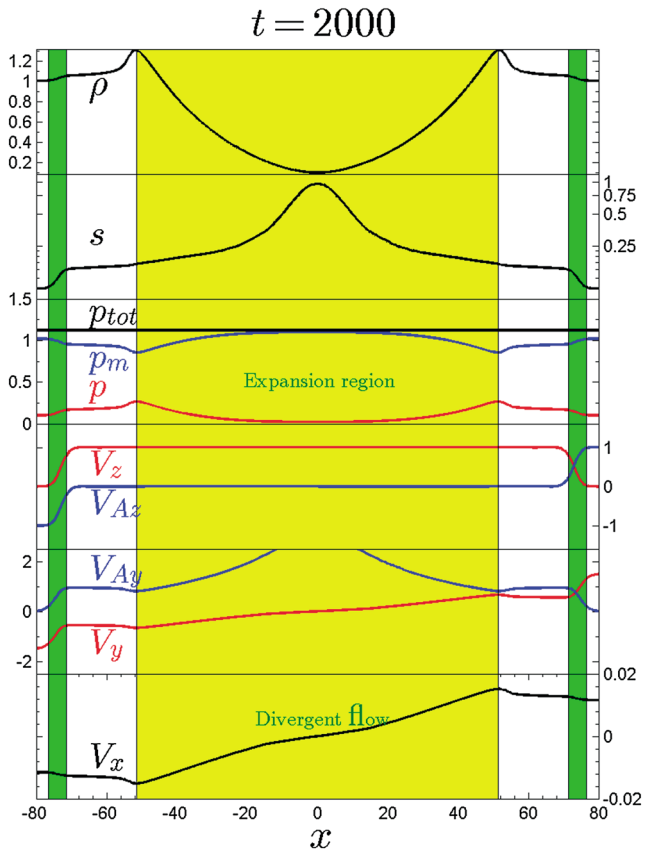

Figure 8. Same as Figure 4 except that it shows the reconnection layer for a supercritical perpendicular sheared flow (i.e., $V_s = 1.5$) from one-dimensional simulation.

expansion region without the influence of the depletion layer, because the specific entropy cannot decrease (i.e., there is no nonadiabatic cooling term), which, consequently, requires density must decrease with thermal pressure. The specific entropy increases by a factor of 4 in the expanded entropy structure; however, this is an artifact of the initial equilibrium condition explained for the reference case.

Figure 9 presents the projection of selected reconnected magnetic field lines in the *xy* plane, which are traced from $x = 0, z = 30$ at $t = 160$ for $V_s = 0.5$ (blue) and 1.5 (red) cases. It shows that the magnetic field lines are strongly bent along the *y* direction due to the sheared flow. The displacement of the magnetic footprints at the *z* boundary, Δy, is roughly proportional to the sheared flow, that is, $\Delta y = 2V_s\Delta t$, where Δt is the interval between the time that the magnetic field was reconnected and the time that the magnetic field is traced. The red line has a displacement of over 140, which is over 3 times that of the blue line. This implies that the red line is reconnected slightly earlier than the blue line. The blue line has a steep slope within $|x| < 2$, indicating that a strong magnetic B_y component is localized in a narrow outflow region. Note that B_y is approximately 0.5 for the reference case because the change of B_y is approximately Alfvénic and the sheared flow has a magnitude of 0.5. The steeper slope of the red line represents an even larger magnetic B_y component, being limited by the total pressure balance. The magnetic field B_y component is approximately 1 in the outflow region because of total pressure balance. However, if the reconnection layer structure for the supercritical flow case were the same as for the reference case, the Walén relation would require a magnetic field of 1.5 in the outflow region. This contradiction also provides the explanation for the presence of a fast expansion region which ensures that approximate total pressure balance is maintained in the reconnection jet.

Figure 10 shows the magnetic reconnection rate, *r*, for $V_s = 1.5$ (red) and $V_s = 0.5$ (blue) cases. Here the reconnection rate is estimated by the difference of the electric field E_y component between the X and O points, that is,

$$r = \eta j_y|_x - \eta j_y|_o, \tag{3}$$

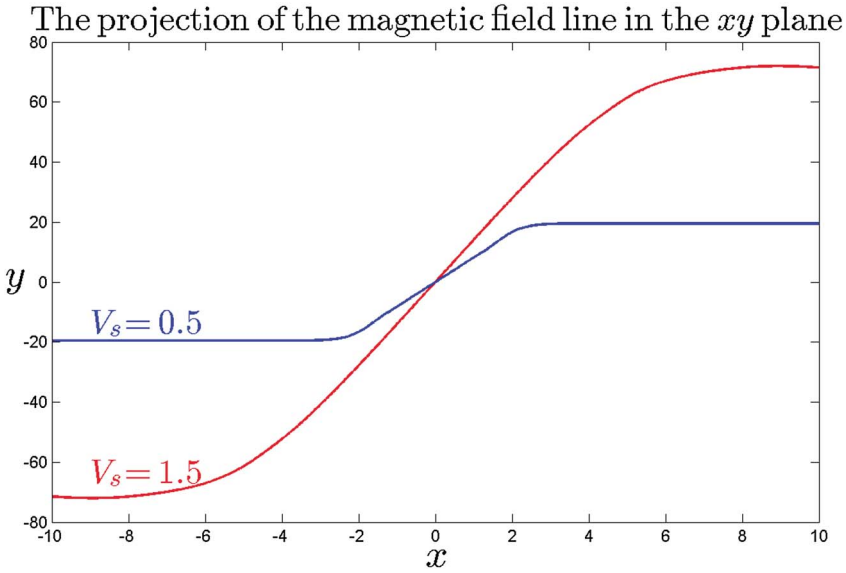

Figure 9. The projection of magnetic field lines in the *xy* plane, being traced from $x = 0$, $z = 30$ for $V_s = 0.5$ (blue) and 1.5 (red) at $t = 160$.

where $B_x = B_z = 0$ at the X and O points and η is the resistivity and j_z is the current density *z* component. The reconnection rate represents how fast the magnetic flux is transported into the outflow region. As such, the divergent flow in the expansion region is expected to significantly reduce the reconnection rate, which is illustrated by Figure 10. It shows that the reconnection rate for $V_s = 0.5$ is about 0.07, being close to the Petschek reconnection rate [*Petschek*, 1964], while the reconnection rate for $V_s = 1.5$ case is only about half of this value. We note that often the reconnection rate is given by the separatrix angle; thus, a wider outflow region appears to indicate a higher reconnection rate. However, a rather large separatrix angle can significantly reduce the current density at the X point, and the net result is a lower reconnection rate. We remind the reader that the expansion region in the outflow region does not satisfy usual reconnection layer assumptions.

3.2. Reconnection With Surface Wave

The prior results ignore the influence of a supercritical sheared flow in the third dimension, which is possible to be Kelvin-Helmholtz unstable during the reconnection process. In order to examine this influence

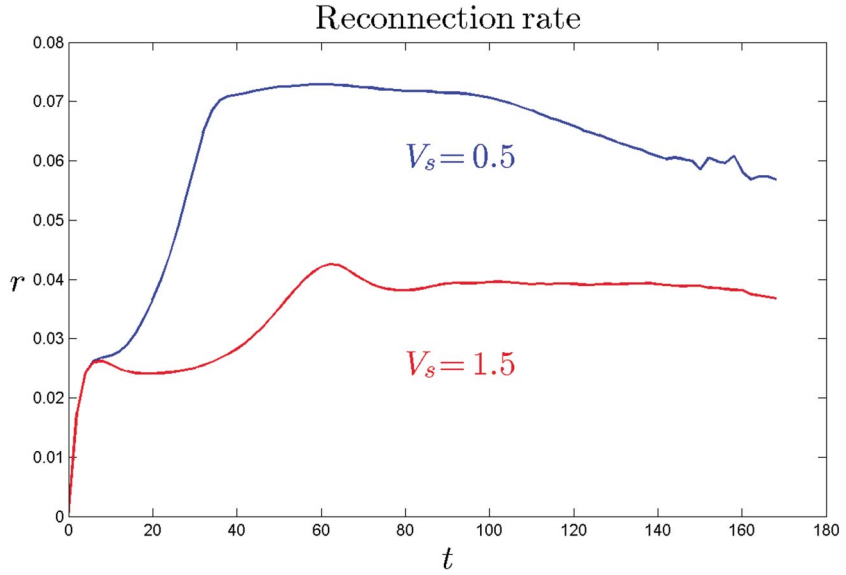

Figure 10. Reconnection rate for $V_s = 0.5$ (blue) and 1.5 (red) cases.

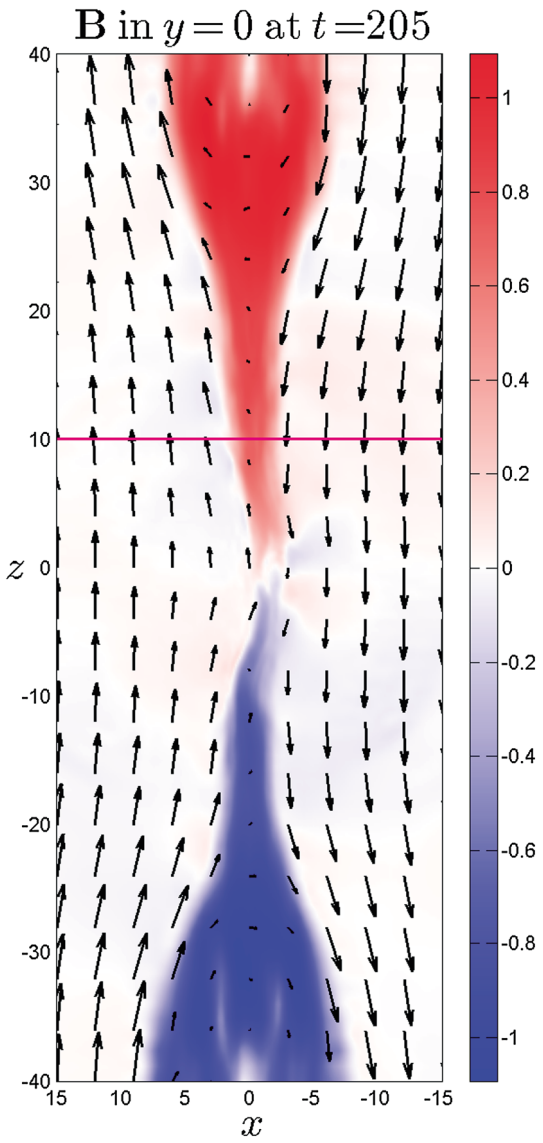

Figure 11. The color index is the magnetic B_y component at $y = 0$ plane at $t = 205$ for the three-dimensional simulation of magnetic reconnection with a supercritical perpendicular sheared flow (i.e., $V_s = 1.5$). Black arrows represent the magnetic B_x and B_z components. Magenta line indicates the place that cut is taken in Figure 13.

we consider a three-dimensional simulation of a case with a supercritical perpendicular sheared flow (i.e., $V_s = 1.5 > V_c = \sqrt{V_{Ai}^2 + (2/\gamma)C_{si}^2}$). Figure 11 represents the magnetic B_y component in $y = 0$ plane by color index and indicates the in-plane magnetic field components by black arrows for the three-dimensional simulation, showing that magnetic reconnection is fully developed at $t = 205$. Figure 12 shows plasma density (color index) and in-plane bulk velocity (black arrows) in $z = 10$, showing that a density depletion layer is separated by a pair of compression layers from the inflow region, which is similar to the two-dimensional configuration.

It is noticeable that these layers have a wave structure with a wavelength about half of the simulation size along the y direction, likely caused by the surface wave. Such surface waves also modify the inflow region, generating some compressional regions (red patchy). It is, therefore, important to consider whether these surface waves will become unstable.

The presence of the reconnection layer modulates the sheared flow profile to a three-layer structure (i.e., inflow-outflow-inflow). The system can be KH unstable at the boundary between inflow and outflow regions,

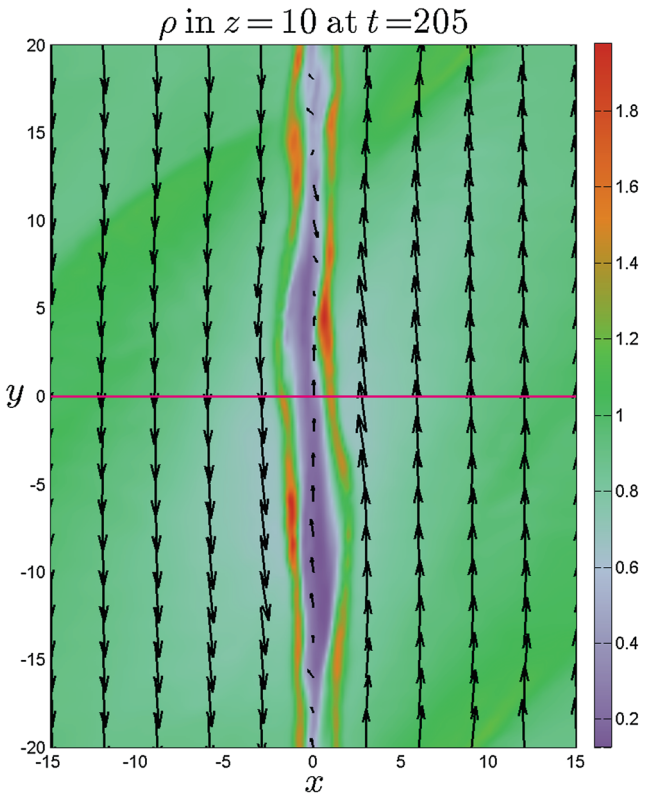

Figure 12. The color index is the plasma density at $z = 10$ and at $t = 205$ for the three-dimensional simulation of magnetic reconnection with a supercritical perpendicular sheared flow (i.e., $V_s = 1.5$). The arrows represent the bulk velocity V_x and V_y components. Magenta line indicates the place that cut is taken in Figure 13.

(i.e, RD/TDIS) and also be KH unstable for the whole three-layer structure, which appears like the kink or sausage mode. Thus, we need to discuss the stability of the boundary between the inflow and outflow regions as well as the whole three-layer structure.

For the boundary between inflow and outflow regions, the total jump speed is smaller than the fast mode speed, which is expected to be KH unstable. However, the RD/TDIS in the reconnection layer still satisfies the Walén relation, that is, the total bulk velocity change equals the change of the Alfvén velocity. Therefore, the KH mode is stabilized by the magnetic field B_y component in the RD/TDIS.

For the whole three-layer structure, the depletion of density in the expansion region increases the local critical speed. Such a change in the outflow region may have only a minor influence on the KH onset conditions, since the wavelength of KH unstable modes is usually much larger than the width of the sheared flow [*Miura and Pritchett*, 1982]. Meanwhile, the widened sheared flow layer implies an even larger KH wavelength, consequently, requiring a large domain along the z direction [*Ma et al.*, 2014a], which is limited by the curvature of the magnetic field line at the magnetopause. Thus, reconnection with a supercritical perpendicular sheared flow is likely to be KH stable in the three-dimensional magnetopause environment.

Figure 13 illustrates the profiles of a one-dimensional cut at $y = 0$ and $z = 10$ (i.e., magenta line in Figures 11 and 12), showing that the reconnection layer in a three-dimensional configuration is indeed similar the two-dimensional configuration (see Figure 7). The density depletion layer (i.e., yellow shading) is bounded by a pair of narrow compressional layers (i.e., gray shading). The magnetic field has a dip in the compressional layer (i.e., gray shading) and increases in the outflow region (i.e., yellow shading). The whole reconnection layer basically maintains the total pressure balance, and the magnetic field and bulk velocity satisfy the Walén relation, except in the density depletion layer. One can hardly find a divergent bulk velocity V_x component, which is likely due to the modulation of the surface wave.

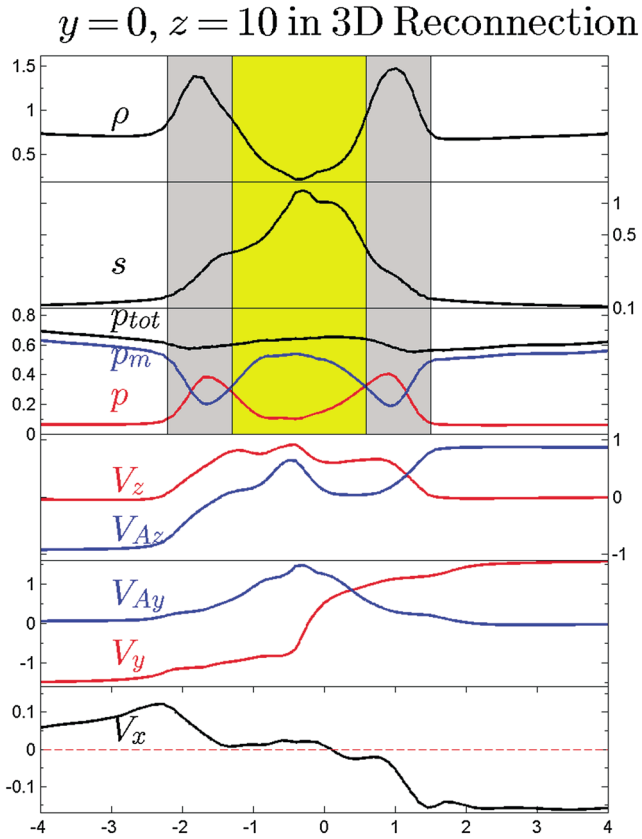

Figure 13. Same as Figure 4 except that it shows profiles of the one-dimensional cut in $y = 0$ and $z = 10$ (i.e., yellow lines in Figures 11 and 12) for the three-dimensional simulation of magnetic reconnection with a supercritical perpendicular sheared flow (i.e., $V_s = 1.5$). The density depletion layer is highlighted by the yellow shading, and magnetic depletion layers are highlighted by the green shading.

4. Discussion

The classical magnetic reconnection layer maintains the total pressure balance and satisfies the Walén relation at same time. This study demonstrated that such magnetic reconnection layer will not exist if the perpendicular sheared flow, V_s, is greater than the critical speed, $V_c = \sqrt{V_{Ai}^2 + (2/\gamma)C_{si}^2}$, due to the contradiction between the Walén relation and the total pressure balance. It is illustrated that a large sheared flow strongly bends the reconnected magnetic field lines to the opposite direction on both sides of the current layer. Such a large displacement requires a strong magnetic field component along the sheared flow direction, which, however, is limited by the total pressure balance. As such, the reconnection outflow region must expand. Thus, the reconnection layer for supercritical perpendicular sheared flow becomes

$$\text{IR} + \text{TDIS/RD} + \text{CL} + \text{ER} + \text{CL} + \text{TDIS/RD} + \text{IR},$$

which is different from the reconnection layer for sub-Alfvénic perpendicular sheared flow [*Lin and Lee*, 1993; *Sun et al.*, 2005], that is,

$$\text{IR} + \text{TDIS/RD} + \text{SS} + \text{TD} + \text{SS} + \text{TDIS/RD} + \text{IR}.$$

Here IR, CL, ER, SS, and TD refer to the inflow region, the compressional layer, the expansion region, the slow shock, and the tangential discontinuity, respectively. The plasma density significantly decreases in this expansion region due to the presence of the divergent normal bulk velocity. The interaction between the divergent flow in the expansion region and convergent flow in the TDIS causes the compressional layer between the TDIS and the expansion region, corresponding to a local minimum magnetic field. It is interesting to notice that the magnitude of the magnetic field increases in the center of the outflow region, opposite to the change for a slow shock. However, for supercritical flow the magnitude of the magnetic field is still smaller than implied

by changes due to the Walén relation. Such changes would require a magnetic field in the outflow region to be larger than the magnetic field in the inflow region which contradicts total pressure balance and necessitates the expansion region, being similar to an expansion wave [*Lin and Lee*, 1993].

The expansion wave conserves the specific entropy [*Lin and Lee*, 1993], while the two-dimensional simulation shows a wide specific entropy enhancement layer in vicinity of the x axis. It is well known that this high specific entropy plasma comes from the diffusion region, and the width of this layer (i.e., density depletion layer) should be close to the width of the diffusion region for reconnection without supercritical perpendicular sheared flow. The divergent flow in the expansion region can increase the width of the density depletion layer. As such, one may expect that the nonadiabatic heating in the diffusion region will become more important because of the larger affected volume. But it is important to notice that the width of the broader density depletion layer can be still small if the width of the diffusion region is on the order of the electron inertia scale. Furthermore, a low reconnection rate indicates less plasma moving into the diffusion region. It should also be mentioned that changes to the flux tube entropy are not clear. Although specific entropy increases and occupies a larger volume, the magnetic field strength increases in the same volume thereby limiting importance of the specific entropy increase for the flux tube entropy.

For the quasi one-dimensional reconnection layer, the induction equation can be written as

$$\frac{\partial B_y}{\partial t} \approx \partial_x (B_x V_y). \tag{4}$$

Taking integral of equation (4) along the x direction from one inflow region through the outflow region and to the other inflow region yields

$$\mathrm{d}\Phi_{\mathrm{out}}/\mathrm{d}t \approx B_x \Delta V_y, \tag{5}$$

where $\Phi_{\mathrm{out}} = \int B_y \mathrm{d}x$ is the magnetic B_y flux in the outflow region. Equation (5) indicates that the perpendicular sheared flow, ΔV_y, and the magnetic B_x component generates magnetic B_y flux in the outflow region. If the sheet does not expand along the x direction, the magnetic B_y component in this sheet just increases as long as the magnetic B_x component and the sheared flow magnitude is constant. This illustrates that for a constant value of the magnetic B_y component in this sheet, the sheet must expand in the x direction with a velocity such that the value of the magnetic B_y component can remain constant despite the magnetic B_y flux generation. In our one-dimensional simulation (i.e., fixed magnetic B_x component), faster shear flow either generates a larger magnetic B_y component or for a fixed magnetic B_y component requires faster expansion in the x direction. In the reconnection geometry (i.e., two- and three-dimensional configuration), time (expansion) translates into distance implying that faster expansion means a larger angle for the outflow region. We note that a smaller magnetic B_x component can also reduce the generation of magnetic B_y flux. In our two-dimensional supercritical cases, the wider reconnection layer indicates a fast expansion of the outflow region, and the lower reconnection rate implies a smaller magnetic B_x component.

It is important to be aware that this study only investigates the simplest idealized model, which misses several important aspects to compare with the actual magnetopause (e.g., the large density and magnetic field asymmetry and anisotropy). For a asymmetric magnetic reconnection configuration, the critical speed on the magnetosheath and magnetospheric sides can be different. As such, the modulation of the traditional reconnection layer structure can still be expected to occur when the total sheared flow jump is greater than the sum of the critical speed on both sides of the current layer, since the causes of this modulation (i.e., fast magnetic flux generation and limitation of magnetic pressure) are independent of configuration symmetry. At the Earth's magnetopause, it is possible that the sheared flow is smaller than the critical speed (i.e., $V_C = \sqrt{V_{Ai}^2 + (2/\gamma)C_{si}^2}$) near the subsolar region. As such, it is interesting to ask whether this reconnection layer structure still exists by considering the influence of the tailward moving KH vortex from the upstream KH unstable region. These important aspects are out of the scope of this paper and, however, deserve a further investigation.

At the Earth's magnetopause, the typical magnetic field in the magnetosheath is about 20 nT, the magnetosheath plasma density is about 10 cm^{-1}, magnetospheric plasma density is about 1 cm^{-1}, and the magnetosheath plasma beta is the order of unity, which yields a critical speed of about 200 km s^{-1} on the magnetosheath side and about 400 km s^{-1} on the magnetospheric side. This means that magnetic reconnection is expected to operate with a supercritical perpendicular sheared flow, if the magnetosheath speed is

over 600 km s^{-1}, which is possible in the flank region [*Dimmock and Nykyri*, 2013]. Another plausible application is the dawn side of Jupiter's and Saturn's magnetopauses, where the magnetic field is much weaker (i.e., about few nT), while the sheared flow increases $\geq$ 200 km s^{-1} due to the corotating magnetodiscs [*Delamere et al.*, 2014].

For the in situ satellite observation, the most prominent observational signature is a magnetic field in the outflow region that is close to the value of the inflow region and the dip of the magnitude of the magnetic field in the density compressional layer. It is expected that the Walén relation is still valid in the RT/TDIS layer; however, the Alfvén speed significantly increases in the expansion layer.

5. Summary

The sheared flow, V_s, at the Earth's magnetopause can be super-Alfvénic and can be often greater than the critical speed (i.e., $V_s > V_c = \sqrt{V_{Ai}^2 + (2/\gamma)C_{si}^2} > V_A$). For magnetic reconnection with a supercritical perpendicular sheared flow, the increase in the magnetic pressure required by the Walén relation cannot be compensated by corresponding decrease in the thermal pressure due to the total pressure balance. As such, the magnetic reconnection layer violates the Walén relation by forming an expansion outflow region, which is fundamentally different from the classical reconnection layer under sub-Alfvénic perpendicular sheared flow conditions. This fast expansion outflow region is characterized by a decrease in plasma density and thermal pressure as well as an increase in the magnitude of the magnetic field. Those features are likely to exist in a three-dimensional geometry and are expected to be plausible in situ observational signatures.

Acknowledgments
The authors acknowledge support from NASA grants NNX15AH09G and NNX13AH30G. The simulation data in this paper can be accessed from the corresponding author at xma2@alaska.edu. We are grateful to the International Space Science Institute (ISSI) for their support to the Coordinated Numerical Modeling of the Global Jovian and Saturnian Systems team. X.M. acknowledges Yixin Hao for inspiring him to design the colormap used in this paper. X.M. thanks Yajie Cao for the suggestion on the color scheme.

References

Birn, J. (1980), Computer studies of the dynamic evolution of the geomagnetic tail, *J. Geophys. Res.*, *85*, 1214–1222, doi:10.1029/JA085iA03p01214.

Cassak, P. A., and A. Otto (2011), Scaling of the magnetic reconnection rate with symmetric shear flow, *Phys. Plasmas*, *18*(7), 074501, doi:10.1063/1.3609771.

Chandrasekhar, S. (1961), *Hydrodynamic and Hydromagnetic Stability, The Int. Ser. of Monogr. on Phys.*, Dover, New York.

Chen, Q. (1997), Two- and three-dimensional study of the Kelvin-Helmholtz instability, magnetic reconnection and their mutual interaction at the magnetospheric boundary, PhD thesis, Univ. of Alaska Fairbanks, Fairbanks.

Chen, Q., A. Otto, and L. C. Lee (1997), Tearing instability, Kelvin-Helmholtz instability, and magnetic reconnection, *J. Geophys. Res.*, *102*, 151–162, doi:10.1029/96JA03144.

Delamere, P. A., F. Bagenal, C. Paranicas, A. Masters, A. Radioti, B. Bonfond, L. Ray, X. Jia, J. Nichols, and C. Arridge (2014), Solar wind and internally driven dynamics: Influences on magnetodiscs and auroral responses, *Space Sci. Rev.*, *187*(1), 51–97, doi:10.1007/s11214-014-0075-1.

Dimmock, A. P., and K. Nykyri (2013), The statistical mapping of magnetosheath plasma properties based on THEMIS measurements in the magnetosheath interplanetary medium reference frame, *J. Geophys. Res. Space Physics*, *118*, 4963–4976, doi:10.1002/jgra.50465.

Fairfield, D. H., A. Otto, T. Mukai, S. Kokubun, R. P. Lepping, J. T. Steinberg, A. J. Lazarus, and T. Yamamoto (2000), Geotail observations of the Kelvin-Helmholtz instability at the equatorial magnetotail boundary for parallel northward fields, *J. Geophys. Res.*, *105*, 21,159–21,174, doi:10.1029/1999JA000316.

La Belle-Hamer, A. L., A. Otto, and L. C. Lee (1995), Magnetic reconnection in the presence of sheared flow and density asymmetry: Applications to the Earth's magnetopause, *J. Geophys. Res.*, *100*, 11,875–11,889, doi:10.1029/94JA00969.

Lin, Y., and L. C. Lee (1993), Structure of reconnection layers in the magnetosphere, *Space Sci. Rev.*, *65*, 59–179, doi:10.1007/BF00749762.

Lin, Y., and L. C. Lee (1999), Reconnection layers in two-dimensional magnetohydrodynamics and comparison with the one-dimensional Riemann problem, *Phys. Plasmas*, *6*, 3131–3146, doi:10.1063/1.873553.

Ma, X., and A. Otto (2013), Mechanisms of field-aligned current formation in magnetic reconnection, *J. Geophys. Res. Space Physics*, *118*, 4906–4914, doi:10.1002/jgra.50457.

Ma, X., and A. Otto (2014), Nonadiabatic heating in magnetic reconnection, *J. Geophys. Res. Space Physics*, *119*, 5575–5588, doi:10.1002/2014JA019856.

Ma, X., A. Otto, and P. A. Delamere (2014a), Interaction of magnetic reconnection and Kelvin-Helmholtz modes for large magnetic shear: 1. Kelvin-Helmholtz trigger, *J. Geophys. Res. Space Physics*, *119*, 781–797, doi:10.1002/2013JA019224.

Ma, X., A. Otto, and P. A. Delamere (2014b), Interaction of magnetic reconnection and Kelvin-Helmholtz modes for large magnetic shear: 2. Reconnection trigger, *J. Geophys. Res. Space Physics*, *119*, 808–820, doi:10.1002/2013JA019225.

Ma, Z. W., and A. Bhattacharjee (2001), Hall magnetohydrodynamic reconnection: The geospace environment modeling challenge, *J. Geophys. Res.*, *106*, 3773–3782, doi:10.1029/1999JA001004.

Miura, A., and P. L. Pritchett (1982), Nonlocal stability analysis of the MHD Kelvin-Helmholtz instability in a compressible plasma, *J. Geophys. Res.*, *87*, 7431–7444, doi:10.1029/JA087iA09p07431.

Nakamura, T. K. M., M. Fujimoto, and A. Otto (2006), Magnetic reconnection induced by weak Kelvin-Helmholtz instability and the formation of the low-latitude boundary layer, *Geophys. Res. Lett.*, *33*, L14106, doi:10.1029/2006GL026318.

Nakamura, T. K. M., M. Fujimoto, and A. Otto (2008), Structure of an MHD-scale Kelvin-Helmholtz vortex: Two-dimensional two-fluid simulations including finite electron inertial effects, *J. Geophys. Res.*, *113*, A09204, doi:10.1029/2007JA012803.

Nykyri, K., and A. Otto (2001), Plasma transport at the magnetospheric boundary due to reconnection in Kelvin-Helmholtz vortices, *Geophys. Res. Lett.*, *28*, 3565–3568, doi:10.1029/2001GL013239.

Nykyri, K., and A. Otto (2004), Influence of the Hall term on KH instability and reconnection inside KH vortices, *Ann. Geophys.*, *22*, 935–949, doi:10.5194/angeo-22-935-2004.

Nykyri, K., A. Otto, B. Lavraud, C. Mouikis, L. M. Kistler, A. Balogh, and H. Rème (2006), Cluster observations of reconnection due to the Kelvin-Helmholtz instability at the dawnside magnetospheric flank, *Ann. Geophys.*, *24*, 2619–2643, doi:10.5194/angeo-24-2619-2006.

Otto, A. (1990), 3D resistive MHD computations of magnetospheric physics, *Comput. Phys. Commun.*, *59*, 185–195, doi:10.1016/0010-4655(90)90168-Z.

Otto, A., and D. H. Fairfield (2000), Kelvin-Helmholtz instability at the magnetotail boundary: MHD simulation and comparison with Geotail observations, *J. Geophys. Res.*, *105*, 21,175–21,190, doi:10.1029/1999JA000312.

Otto, A., J. Büchner, and B. Nikutowski (2007), Force-free magnetic field extrapolation for MHD boundary conditions in simulations of the solar atmosphere, *Astron. Astrophys.*, *468*, 313–321, doi:10.1051/0004-6361:20054495.

Petschek, H. E. (1964), Magnetic field annihilation, in *The Physics of Solar Flares, NASA Spec. Publ.*, vol. 50, edited by W. N. Hess, pp. 425–439, NASA, Washington, D. C.

Potter, D. (1973), *Computational Physics*, Wiley, New York.

Sun, X., Y. Lin, and X. Wang (2005), Structure of reconnection layer with a shear flow perpendicular to the antiparallel magnetic field component, *Phys. Plasmas*, *12*(1), 012305, doi:10.1063/1.1826096.

Walén, C. (1944), On the theory of sunspots, *Ark. Astron.*, *30*, 1–87.